JACS
JOURNAL OF THE AMERICAN CHEMICAL SOCIETY

Article

pubs.acs.org/JACS

Open Access on 01/13/2015

Generalized Platform for Antibody Detection using the Antibody Catalyzed Water Oxidation Pathway

M. Elizabeth Welch,[†,‡] Nicole L. Ritzert,[†] Hongjun Chen,[†] Norah L. Smith,[†] Michele E. Tague,[†] Youyong Xu,[‡] Barbara A. Baird,[†] Héctor D. Abruña,[†] and Christopher K. Ober*[,‡]

[†]Department of Chemistry and Chemical Biology, Cornell University, 122 Baker Laboratory, Ithaca, New York 14853, United States
[‡]Department of Materials Science and Engineering, Cornell University, 310 Bard Hall, Ithaca, New York 14853, United States

Supporting Information

ABSTRACT: Infectious diseases, such as influenza, present a prominent global problem including the constant threat of pandemics that initiate in avian or other species and then pass to humans. We report a new sensor that can be specifically functionalized to detect antibodies associated with a wide range of infectious diseases in multiple species. This biosensor is based on electrochemical detection of hydrogen peroxide generated through the intrinsic catalytic activity of all antibodies: the antibody catalyzed water oxidation pathway (ACWOP). Our platform includes a polymer brush-modified surface where specific antibodies bind to conjugated haptens with high affinity and specificity. Hydrogen peroxide provides an electrochemical signal that is mediated by Resorufin/Amplex Red. We characterize the biosensor platform, using model anti-DNP antibodies, with the ultimate goal of designing a versatile device that is inexpensive, portable, reliable, and fast. We demonstrate detection of antibodies at concentrations that fall well within clinically relevant levels.

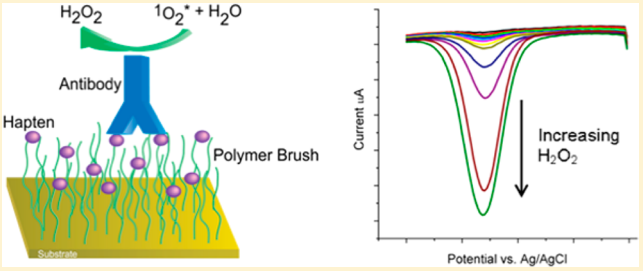

Detection of antibodies is a primary tool for diagnosing infectious diseases. Pandemics, which originate in other species and then jump to humans, represent a particular threat. Influenza pandemics have occurred every 10−50 years from as early as 1580 with tragic consequences on human and livestock populations and their economies.[1] The avian H5N1 influenza, which probably originated in migratory waterfowl, infected domestic chickens with high mortality rates.[2] Although transfer to humans initially appeared to be limited to direct interactions, recent reports show that this virus potentially can be transmitted by aerosol or respiratory droplets between mammals.[3] With escalating world population and global mobility, the challenges of preventing flu and other epidemics from proliferating are increasingly difficult. Significantly improved detection of these diseases, as they transfer through species, would aid substantially in providing early warning of these threats.[2] When a viral or other pathogenic infection is met by an immune response, antibodies are generated that are specific for chemical groups (haptens) on proteins or other pathogen components (antigens), and hence early discovery is often most easily accomplished by detection of these antibodies. Although sensitive antibody detection methods are currently available, they have limitations, and reliable new technologies are needed to meet the demand for rapid detection of highly contagious infections in humans and other species, especially in locations with limited laboratory access.

The importance of antibody detection extends well beyond disease diagnosis and includes development of therapeutic monoclonal antibodies as well as experimental biology of many types. Currently, the most widely used methods for antibody detection are based on the enzyme-linked immunosorbent assay (ELISA). Selected haptenic groups are immobilized on a surface, followed by addition of a sample (e.g., blood serum) potentially containing antibodies, which bind to the hapten.

Detection of these immobilized antibodies is carried out using a specially prepared secondary reagent, most often a secondary antibody specific for the analyte antibody class (e.g., IgG). The secondary antibody is labeled with a tag such as a fluorescent molecule or an enzyme producing a colorimetric substrate. Requiring a secondary reagent increases the number of analytical and incubation steps and thus increases both the analysis time and the risk of nonspecific binding, leading to false positives.

To overcome the limitations of the ELISA method, we have developed a sensor platform based on the antibody-catalyzed water oxidation pathway (ACWOP) that takes advantage of the intrinsic capacity of single antibodies to catalyze the production of hydrogen peroxide (H_2O_2) from water in the presence of singlet oxygen ($^1O_2$*), which can be generated by a photosensitizer (Figure 1). Wentworth et al. first described the ACWOP and showed that it is independent of specificity, class, and species of antibody.[4] The structural locus of this novel activity was found to be in the constant regions of immunoglobulins.[5] The catalytic activity produces multiple

Received: September 17, 2013
Published: January 13, 2014

 © 2014 American Chemical Society dx.doi.org/10.1021/ja409598c | J. Am. Chem. Soc. 2014, 136, 1879−1883

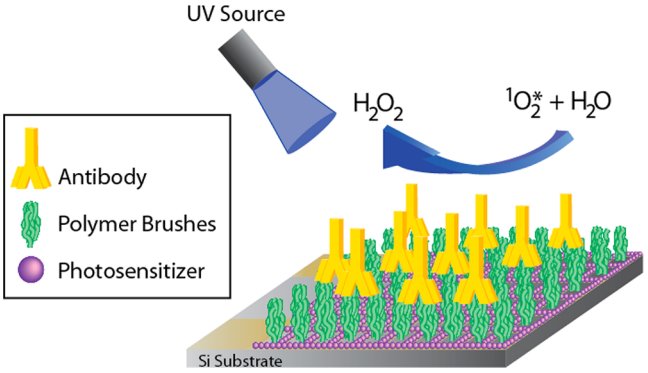

Figure 1. Schematic of biosensor platform based on the ACWOP process.

mole equivalents of H_2O_2 per antibody (reportedly up to 40, or up to 500 if the product is continuously removed) to reach levels that can be detected and quantified using fluorescence in a biochemical assay.[6] We confirmed the previous fluorescence method of ACWOP detection and have now successfully detected antibody generated H_2O_2 using electrochemical methods.[6,7] A primary advantage of the ACWOP is that it allows for the direct detection of antibodies, via H_2O_2, regardless of the antibodies' species and specificity, eliminating the need for specially prepared secondary reagents and mitigating other limitations of the ELISA approach. Our ultimate goal is to create a portable microfluidic platform for sensitive, rapid, and inexpensive detection of antibodies. Herein, we report key results toward fabricating and testing such a device.

RESULTS AND DISCUSSION

Our device incorporates three key elements: patterned polymer brushes to present selected haptenic groups; cofactors required for ACWOP; and components for electrochemical detection and quantification of H_2O_2 (Figure 1). Details about the materials and methods used and additional control experiments are given in the Supporting Information. A fundamental feature of our device is the use of poly(oligoethylene glycol methacrylate) (POEGMA) polymer brushes (Figure 2A) for anchoring a variety of hapten groups and for preventing nonspecific adsorption of other biomolecules that may be present in the test sample. OEG moieties are known to be resistant to protein adsorption and have long-term stability.[8] This is due to the dense packing of neighboring chains which results in an increased entropic force and drives the brushes into a stretched state at high grafting densities to yield effective resistance to nonspecific binding.[9] To produce the necessary high grafting density, we employed atom transfer radical polymerization (ATRP) methods to grow brushes on either a silicon wafer chip or a gold-plated quartz crystal microbalance (QCM) crystal.[10] By functionalizing the initiator end with either a silane or thiol group, we selectively bind the polymer brushes to silicon or gold surfaces, respectively. Polymer brushes have the capacity to be modified with a broad range of haptens for corresponding detection of antibodies with a broad range of specificities.

For initial development and optimization of this platform, we used 2,4-dinitrophenyl (DNP) groups as a model hapten. This well-characterized hapten binds specific anti-DNP antibodies of several classes and species and can be conjugated to the ends of the brushes through a one-step process (Figure 2A). The

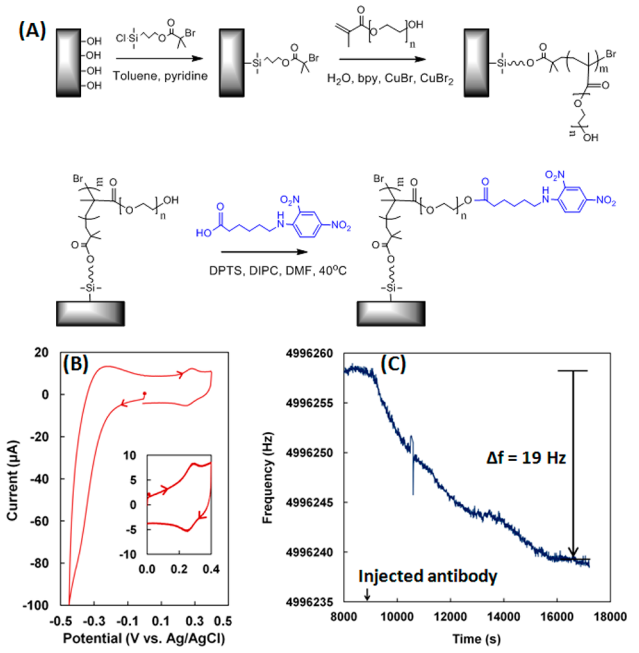

Figure 2. (A) Synthesis of polymer brushes on a silicon substrate. Gold surface modification using thiol based initiators was also carried out. (B) Cyclic voltammogram of DNP-functionalized polymer brush. Inset: Cyclic voltammogram of hydroxylamine formed upon reducing DNP. Supporting electrolyte, 0.1 M H_2SO_4; sweep rate, 100 mV/s. (C) Frequency response of QCM crystal platform in PBS, pH 7.2, containing 1 mg/mL BSA solution at 25 °C. Rat anti-DNP IgG antibody solution (resultant concentration 11 nM) was added at 9000 s.

functionalized polymer brushes ranged in thickness from 13 to 35 nm, measured via ellipsometry, and two methods were utilized to confirm the presence of DNP groups. First, fluorescence imaging with fluorescently labeled anti-DNP IgG antibodies verified the presence of the DNP groups when compared to a sample of unfunctionalized brushes (Supporting Information Figure S1). Second, DNP is electroactive, allowing measurement of its surface coverage through cyclic voltammetry by means of the reduction of nitro groups to the corresponding hydroxylamine (Figure 2B). The surface coverage of DNP was typically on the order of 10^{-11} mol/cm^2, and as high as 1.5×10^{-10} mol/cm^2.

Quartz crystal microbalance (QCM) measurements were used to determine the surface coverage of the antibodies (Figure 2C). The functionalized QCM crystal was placed in phosphate-buffered saline solution (PBS, pH 7.2), and the frequency was allowed to stabilize before the addition of a solution containing anti-DNP IgG antibodies (Figure 2C). Acoustic impedance methods (Supporting Information Figure S2) confirmed that the films were rigid, and the Sauerbrey equation was used to relate the change in frequency to the mass of immobilized antibodies.[11] The antibody surface coverage was typically $5(\pm 2) \times 10^{-12}$ mol/cm^2. The POEGMA brushes were tested for nonspecific adsorption in control experiments by incubating the QCM crystals modified with POEGMA-DNP in a solution of nonspecific antibodies. No significant change in the frequency was observed (Supporting Information Figure S2), confirming that nonspecific antibodies do not bind to the brushes. Furthermore, no significant increase in the amount of H_2O_2 was observed under these control conditions (vide infra) (Supporting Information Figure S3).

dx.doi.org/10.1021/ja409598c | J. Am. Chem. Soc. 2014, 136, 1879−1883

Two types of platforms were used, one on silicon and another on a QCM crystal, in both cases presenting the polymer brushes adjacent to the photosensitizer on the same surface (Figure 3A and B). Our ultimate device is designed to

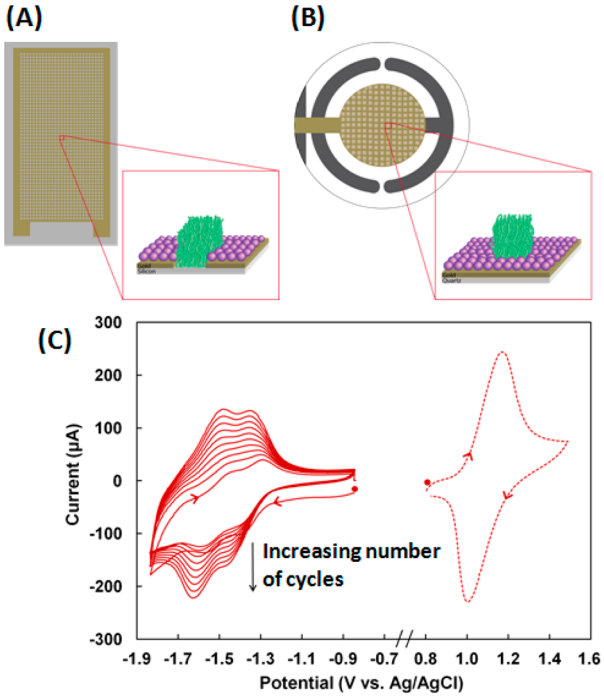

Figure 3. (A, B) Grid patterns of 150 μm wide lines surrounding 300 × 300 μm^2 square areas on silicon (A) and gold electrode of a QCM crystal (B). Note that the figure is not drawn to scale. (C) Cyclic voltammograms of photosensitizer. Solid lines are for QCM crystal platform immersed in 0.5 mM $[Ru(v\text{-}bpy)_3](PF_6)_2$, showing electropolymerization of photosensitizer upon reduction. Dashed lines are for an electropolymerized layer of $[Ru(v\text{-}bpy)_3]^{2+}$ in fresh solution. Supporting electrolyte, 0.1 M $TBAPF_6$ in MeCN; sweep rate, 100 mV/s.

employ silicon chips. However, for calibration purposes, QCM crystals were used to quantify the mass of the bound antibodies. For the silicon chips, gold was evaporated onto 1 × 2 cm^2 silicon wafer pieces in a grid pattern. The photosensitizer was electropolymerized on the gold (vide infra), whereas the polymer brushes, grown as depicted in Figure 2A, were confined to the silicon oxide squares (Figure 3A). The same grid pattern was used for a QCM crystal (Figure 3B). However, because both the polymer brushes and photosensitizer were polymerized from a gold surface on the QCM crystal, a series of steps was employed to prevent the two films from overlapping. First, a photoresist was spin coated onto the QCM crystals, exposed and developed to pattern the grid. Next, the thiol functionalized ATRP initiator was immobilized on the exposed gold surface, and the photoresist was subsequently removed. Finally, the photosensitizer was electropolymerized on the sections where the photoresist was removed, and polymer brushes were then grown from the regions containing the immobilized ATRP initiator. This specific order of patterning and immobilization of the different components allowed for the maximum yield of both photosensitizer and polymer brushes on the same surface.

As described above, the ACWOP process requires singlet oxygen, $^1O_2$*, which can be generated from ambient oxygen $^3O_2$ through the use of a photosensitizer, such as $[Ru(4\text{-vinyl-}4'\text{-methyl-}2,2'\text{-bipyridine})_3]^{+2}$ ($[Ru(v\text{-}bpy)_3]^{+2}$). We found that electropolymerized films of $[Ru(v\text{-}bpy)_3]^{+2}$ (Figure 3C)[12] on the gold electrode immediately adjacent to the brushes maximized production of H_2O_2. Typical coverage of photosensitizer was 1.5(±0.5) × 10^{-9} mol/cm^2, corresponding to a thickness of ca. 26 nm. In addition to enhancing the signal-to-noise ratio, our results showed a significant increase in the ACWOP H_2O_2 signal for the adjacent, immobilized photosensitizer compared to photosensitizer in solution. This increase is likely the result of having the singlet oxygen generated in close proximity to the antibody. The lifetime of singlet oxygen in aqueous solution is in the range 1−10 μs corresponding to a mean square distance (MSD) diffusion of less than 0.5 μm, assuming a diffusion coefficient of 2 × 10^{-5} cm^2/s.[13] Generating the singlet oxygen in close proximity to the antibody clearly enhances the sensitivity of the biosensor. During the course of developing this biosensor we tested a number of other photosensitizers, including those used previously in ACWOP experiments,[4] and we found these to be suboptimal. While there may be more efficient singlet oxygen sensitizers in solution, in our view $[Ru(4\text{-vinyl-}4'\text{-methyl-}2,2'\text{-bipyridine})_3]^{+2}$ represents an almost ideal sensitizer in that it can be readily polymerized, giving rise to the above-mentioned proximity advantage, and the resulting films are conformal and quite robust. These are most important and attractive attributes when considering field deployment. Moreover, the complex is easily synthesized and purified, and solutions can be used multiple times.

To generate $^1O_2$*, and consequently H_2O_2, the QCM crystal containing the immobilized antibodies and electropolymerized sensitizer was immersed in 3 mL of PBS (pH 7.2) and exposed to UV irradiation for 60 min. We found that 60 min with a broad wavelength source was optimal, as longer exposure times resulted in a decrease in signal and increase in background, possibly due to UV damage of the antibody (Supporting Information Figure S4).

The H_2O_2 generated was quantified using square-wave voltammetry (SWV) (Figure 4), which provides high sensitivity at low analyte concentrations.[6,7,14] Amplex Red (*N*-acetyl-3,7-dihydrophenoxazine) reacts with H_2O_2 in a 1:1 ratio in the presence of horseradish peroxidase (HRP) to produce resorufin (7-hydroxy-3*H*-phenoxazin-3-one), which is fluorescent and also exhibits a reversible redox response.[15] The lowest concentration of H_2O_2 detected with SWV was 0.33 nM (Figure 4A,B).

Assuming a surface coverage of antibodies of 5 × 10^{-12} mol/cm^2, and a liquid thickness of 100 μm (a value readily achievable in a microfluidic platform), a single turnover per immobilized antibody would give rise to a peroxide concentration of 500 nM, clearly well above our detection limit (less than 0.5 nM). In comparative measurements we confirmed that SWV detection is much more sensitive than the fluorescence assay (Supporting Information Figure S5).

To quantify the number of mole equivalents of H_2O_2 generated per antibody, we evaluated H_2O_2 produced in the presence and absence of the immobilized antibody (Figure 4C). An aliquot of the irradiated solution was diluted with pH 6.0 PBS, followed by addition of Amplex Red and HRP. SWV was used to measure the amount of resorufin, which reduces near −0.2 V versus Ag/AgCl, at a glassy carbon electrode. A readily quantifiable increase in reduction current (i.e., the amount of H_2O_2 produced) resulted from the presence of adsorbed

dx.doi.org/10.1021/ja409598c | *J. Am. Chem. Soc.* 2014, 136, 1879−1883

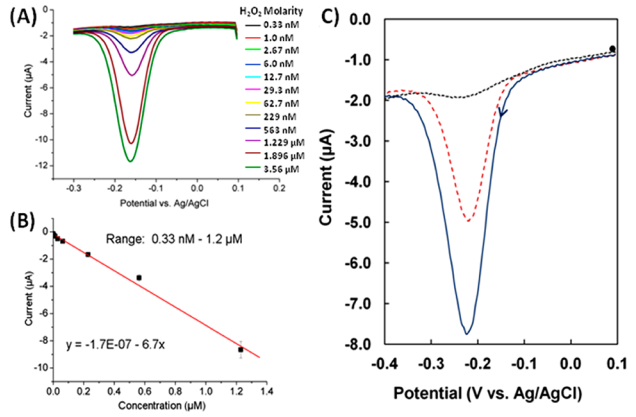

Figure 4. (A) Square wave voltammetry of 10 μM Amplex Red and 0.2 U/mL horseradish peroxidase (HRP) with varying concentrations of H_2O_2 to construct a (B) calibration curve. Supporting electrolyte was PBS, pH 6.0. Step size, 5 mV; amplitude, 25 mV; frequency, 25 Hz. (C) Square wave voltammograms showing detection of H_2O_2 via reduction of resorufin at a 3 mm glassy carbon working electrode after irradiation of the immunosensor's surface with UV light. Black short dashed line is 10 μM Amplex Red; red long dashed line is 10 μM Amplex Red with 0.2 U/mL HRP in the absence of antibody; blue solid line is 10 μM Amplex Red with 0.2 U/mL HRP in the presence of adsorbed antibody. Step size, 5 mV; amplitude, 25 mV; frequency, 25 Hz. A 1.5 mL aliquot of each irradiated solution in PBS, pH 7.2, was diluted to 5.0 mL using PBS, pH 6.0, and then Amplex Red and HRP solutions were added after deaerating the PBS. Square wave voltammetry was subsequently carried out.

antibody. Using a calibration curve, the mole ratio of H_2O_2 produced per antibody was determined. (Figure 4A,B). The ratio of H_2O_2 per antibody was 640−1200, which substantially exceeds the previously reported values.[6] Although this difference may be due, in part, to an increase in temperature, the biggest influence may be the generation of $^1O_2$* in close proximity to the antibody (*vide supra*), such that this highly reactive species is more readily intercepted by the antibody to generate H_2O_2. For any particular application, further calibration with reference antibody stocks will allow the concentration of antibodies in the test sample to be determined.

CONCLUSION

In summary, we have developed a general immunobiosensor platform, employing patterned polymer brushes with photosensitizer films, based on the electrochemical detection of H_2O_2 at clinically relevant concentrations generated through the ACWOP. We have shown that H_2O_2 at concentrations as low as 0.33 nM can be measured in a biosensor device. Antibodies at a surface coverage of 5×10^{-12} mol/cm^2 generate more than 25×10^{-10} mol H_2O_2/cm^2 (or >250 μM H_2O_2, assuming a volume of 1 cm × 1 cm × 100 μm) in 60 min. However, H_2O_2 can be readily quantified well below this concentration (see Figure 4A), and our tests indicate that this device can detect less than 3 pg antibodies in a 10 μL sample (2 pM). This compares quite favorably to the most sensitive ELISAs, which require secondary agents and additional procedural steps. As for the ELISA, a challenge is to ensure sufficiently high signal-to-noise, which can be limited by nonspecific antibody binding. The POEGMA brushes in our platform appear to excel in this regard, and we will continue to develop these as we test samples including high concentrations of nonspecific antibodies, resembling typical blood serums. Eliminating the use of secondary antibodies, as in the case of ELISA, reduces the chances for nonspecific "false positives" and furthermore makes our platform appealing for low cost applications. Moreover, since the ACWOP is a general characteristic of antibodies, our approach can, in principle, be applied to antibodies of virtually any specificity, class, or species. We found results obtained from antibodies adsorbed on the platform on a silicon chip to be similar to those obtained using the QCM crystal (Supporting Information Figure S6). We are currently exploring the incorporation of this approach into a microfluidic platform, which would expedite wash steps to minimize nonspecific binding, as well as delivery of the final test solution for SWV measurement of H_2O_2 concentration in a separate part of the device. In the long run this device may also be useful for quantitatively assessing affinities of specific antibodies in a way not possible with ELISAs because of their need for secondary antibodies that complicate the binding analysis. Such a microfluidic platform, in combination with flexible electronics (again recall that [Ru(4-vinyl-4′-methyl-2,2′-bipyridine)$_3$]$^{+2}$ can be electropolymerized as conformal films) should eventually facilitate widespread use and field deployment.

ASSOCIATED CONTENT

Supporting Information

Details of materials, synthesis and sample preparation, measurement of DNP, device fabrication, nonspecific antibody adsorption, electrochemical polymerization of photosensitizer, optimization of exposure time, SWV comparison to fluorescent measurements, temperature measurements, hydrogen peroxide generation on Si chip. This material is available free of charge via the Internet at http://pubs.acs.org.

AUTHOR INFORMATION

Corresponding Author

cko3@cornell.edu

Author Contributions

The manuscript was written through contributions of all authors. All authors have given approval to the final version of the manuscript.

Notes

The authors declare no competing financial interest.

ACKNOWLEDGMENTS

We acknowledge support by NSF Grant DMR-1105253. Work supported in part by Grants NSF-NBTC ECS-9876771 and NIH R01AI18306. This work made use of the Nanobiotechnology Center (NBTC) shared research facilities at Cornell University, and the Cornell NanoScale Facility, a member of the National Nanotechnology Infrastructure Network, which is supported by the NSF (Grant ECS-0335765). Also, Rob Ilic (CNF), Jimmy John, and Roxana Amirahmadi are gratefully acknowledged for their invaluable suggestions and assistance.

REFERENCES

(1) (a) Potter, C. W. *J. Appl. Microbiol.* **2001**, *91*, 572. (b) Burns, A.; van der Mensbrugghe, D.; Timmer, H. *Global Development Finance: The Development Potential of Surging Capital Flows*, The World Bank: Washington, DC, 2006.

(2) (a) Sturm-Ramirez, K. M.; Ellis, T.; Bousfield, B.; Bissett, L.; Dyrting, K.; Rehg, J. E.; Poon, L.; Guan, Y.; Peiris, M.; Webster, R. G.

J. Virol. **2004**, *78*, 4892. (b) Velumani, S.; Ho, H.-T.; He, F.; Musthaq, S.; Prabakaran, M.; Kwang, J. *PLoS One* **2011**, *6*, e20737.
(3) (a) Herfst, S.; Schrauwen, E. J. A.; Linster, M.; Chutinimitkul, S.; de Wit, E.; Munster, V. J.; Sorrell, E. M.; Bestebroer, T. M.; Burke, D. F.; Smith, D. J.; Rimmelzwaan, G. F.; Osterhaus, A.; Fouchier, R. A. M. *Science* **2012**, *336*, 1534. (b) Russell, C. A.; Fonville, J. M.; Brown, A. E. X.; Burke, D. F.; Smith, D. L.; James, S. L.; Herfst, S.; van Boheemen, S.; Linster, M.; Schrauwen, E. J.; Katzelnick, L.; Mosterin, A.; Kuiken, T.; Maher, E.; Neumann, G.; Osterhaus, A.; Kawaoka, Y.; Fouchier, R. A. M.; Smith, D. J. *Science* **2012**, *336*, 1541. (c) Imai, M.; Watanabe, T.; Hatta, M.; Das, S. C.; Ozawa, M.; Shinya, K.; Zhong, G. X.; Hanson, A.; Katsura, H.; Watanabe, S.; Li, C. J.; Kawakami, E.; Yamada, S.; Kiso, M.; Suzuki, Y.; Maher, E. A.; Neumann, G.; Kawaoka, Y. *Nature* **2012**, *486*, 420.
(4) Wentworth, P.; Jones, L. H.; Wentworth, A. D.; Zhu, X. Y.; Larsen, N. A.; Wilson, I. A.; Xu, X.; Goddard, W. A.; Janda, K. D.; Eschenmoser, A.; Lerner, R. A. *Science* **2001**, *293*, 1806.
(5) (a) Zhu, X. Y.; Wentworth, P.; Wentworth, A. D.; Eschenmoser, A.; Lerner, R. A.; Wilson, I. A. *Proc. Natl. Acad. Sci. U.S.A.* **2004**, *101*, 2247. (b) Datta, D.; Vaidehi, N.; Xu, X.; Goddard, W. A. *Proc. Natl. Acad. Sci. U.S.A.* **2002**, *99* (5), 2636−2641.
(6) Lyon, J. L.; Stevenson, K. J. *Anal. Chem.* **2006**, *78*, 8518.
(7) Bard, A. J.; Faulkner, L. R. *Electrochemical Methods: Fundamentals and Applications*, 2nd ed.; Wiley: New York, 2001.
(8) Harder, P.; Grunze, M.; Dahint, R.; Whitesides, G. M.; Laibinis, P. E. *J. Phys. Chem. B* **1998**, *102*, 426.
(9) Wang, R. L. C.; Kreuzer, H. J.; Grunze, M. *J. Phys. Chem. B* **1997**, *101*, 9767.
(10) Senaratne, W.; Takada, K.; Das, R.; Cohen, J.; Baird, B.; Abruna, H. D.; Ober, C. K. *Biosens. Bioelectron.* **2006**, *22*, 63.
(11) Sauerbrey, G. *Z. Phys.* **1959**, *155*, 206.
(12) Abruna, H. D.; Denisevich, P.; Umana, M.; Meyer, T. J.; Murray, R. W. *J. Am. Chem. Soc.* **1981**, *103*, 1.
(13) (a) Salokhiddinov, K. I.; Byteva, I. M.; Gurinovich, G. P. *J. Appl. Spectrosc.* **1981**, *34*, 892. (b) Merkel, P. B.; Kearns, D. R.; Nilsson, R. *J. Am. Chem. Soc.* **1972**, *94*, 1030.
(14) Osteryoung, J. G.; Osteryoung, R. A. *Anal. Chem.* **1985**, *57*, A101.
(15) Gajovic-Eichelmann, N.; Bier, F. F. *Electroanalysis* **2005**, *17*, 1043.